

**Phys Chem Chem Phys 17 (2015) 24045-24055**

**DOI: 10.1039/C5CP03749B**

# Transferable Force Field for Adsorption of Small Gases in Zeolites

*A. Martin-Calvo<sup>1</sup>, J. J. Gutiérrez-Sevillano<sup>1</sup>, J. B. Parra<sup>2</sup>, C.O. Ania<sup>2</sup>, and S. Calero<sup>1\*</sup>*

<sup>1</sup>Department of Physical, Chemical, and Natural Systems, University Pablo de Olavide,  
Ctra. de Utrera, km. 1, 41013 Seville, Spain

<sup>2</sup> Instituto Nacional del Carbón, INCAR-CSIC, P.O. 73, 33080 Oviedo, Spain

\*Correspondence should be addressed to S. Calero ([scalero@upo.es](mailto:scalero@upo.es))

## **Abstract**

We provide transferable force fields for oxygen, nitrogen, and carbon monoxide that are able to reproduce experimental adsorption in both pure silica and aluminosubstituted zeolites at cryogenic and high temperatures. The force field parameters can be combined with those previously reported for carbon dioxide, methane, and argon, opening the possibility of studying mixtures of interest containing the six components. Using these force field parameters we obtained some adsorption isotherms at cryogenic temperatures that at first sight were in discrepancies with experimental values for certain molecules and structures. We attribute these discrepancies to the sensitiveness of the equipment and to kinetic impedimenta that can lead to erratic results. Additional problems can be found during simulations when extra-framework cations are present in the system as their lack of mobility at low temperatures could lead to kinetic effects that hinder experimental adsorption.

## **Introduction**

Despite of the efforts on force field development in the last decades, the lack of transferable parameters to define low temperature adsorption of certain gases in zeolites is still an impeding factor from the simulation point of view. Using molecular simulation as predictive tool requires reliable models as well as effective force fields able to reproduce experimental data. The main difficulty of defining interactions between adsorbates and zeolites is that generic mixing rules fail for these systems.<sup>1-3</sup> Lennard-Jones interactions between different atoms can be computed using Jorgensen or the Lorentz-Berthelot mixing rules. In the former the cross term parameters for energy and distance are calculated by a geometric mean and in the latter the cross-term parameters for energy and distance are calculated by a geometric and arithmetic mean,

respectively. These generic force fields have the advantage of being easy to implement, but, especially at low temperatures, they tend to over predict experimental adsorption<sup>4</sup> and fail to reproduce particular kinks and steps of the adsorption isotherms attributed to differences on the molecular packing at low and high coverage and to phase transitions within the pores.<sup>1-3,5-9</sup> Due to the lack of specific and transferable force fields, generic force fields are still widely used for porous materials. However the development of more accurate force fields (obtained by fitting to experimental measurements) will improve the capacity of molecular simulations to provide reliable predictions about adsorption and diffusion properties of these porous materials. For zeolites some transferable force field potentials (that can be used for a variety of structures) are being developed. However, combining models is just as cumbersome.

To date there are many works describing these interactions but most of them are developed for specific purposes and molecular models and they are not transferable to other structures or to different working conditions. One of the most studied adsorbates in zeolites is carbon dioxide. For this molecule a variety of force fields are reported in the literature in both pure silica<sup>10-13</sup> and alumino-silicate crystals.<sup>14-16</sup> Among these force fields only one of them has been proven to be transferable to all zeolitic topologies, reproducing accurately experimental adsorption under different conditions<sup>8</sup>. Regarding diffusion of carbon dioxide in zeolites, most of the simulation studies focus in pure silica structures<sup>17-21</sup> and it has been demonstrated that small differences on the host-guest parameters lead to similar adsorption but have large influence on diffusion.<sup>22</sup> The adsorption and diffusion of alkanes have also been widely studied in both pure silica and alumino-substituted zeolites.<sup>21,23,24</sup> While the adsorption of hydrocarbons is well reproduced in all-silica zeolites using force fields such as TraPPE<sup>25</sup> or this of Dubbeldam *et al.*,<sup>1</sup> important differences can be found in diffusion studies.<sup>22,26-30</sup> The

adsorption and diffusion of other small gases such as nitrogen, argon, oxygen, or carbon monoxide have also been reported in zeolites but in lesser amount.<sup>9,11,13,17,21,24,31-37</sup>

Despite current efforts, the development of transferable force fields for describing the adsorption in zeolites (especially at low temperatures) remains a complex task. There are two main challenges in fitting a force field to experimental data: The choice of experimental data that are used in the fitting and in the validation steps, and the nature of the parameter fitting method.

In this work we provide a transferable force field for light gases that are able to reproduce experimental adsorption in both pure silica and alumino-substituted zeolites. We rely on reported transferable force fields for argon<sup>9</sup> and methane<sup>1</sup> and we develop new parameters for nitrogen, oxygen, and carbon monoxide to reproduce experimental adsorption in zeolites for a variety of temperatures. One of the particularities of these force fields is that they can be combined with these previously reported for carbon dioxide,<sup>8</sup> argon,<sup>9</sup> and methane.<sup>1</sup> This fact is of high relevance as it makes possible to compute adsorption in zeolites of a variety of mixtures with industrial and environmental impact (i.e. natural gas, tail gases from Fisher Tropsch processes, greenhouse gases, or pollutant removal from air). Usually available force fields are optimized at room temperature, but in this work we fit the force field parameters at 77 K and 120 K (depending on the adsorbate) in order to guarantee their validity for a wider range of temperatures. This fact lead to another particularity of these force field parameters as they can be used to analyze the difficulties faced by both experimentalists and theoreticians to obtain reliable adsorption at low temperature and allow us to point out some factors that can induce to erratic sets of data.

In the next sections we detail the experimental and simulation methodology, we discuss the results obtained, and finally we summarize our main findings of this work.

## **Methodology**

**Experimental details.** Zeolites with faujasite topology were purchased from Zeolyst International (CBV100 and CBV901). All silica MFI (RSIL) and ITQ-29 (pure silica LTA structure) were kindly supplied by ITQ (CSIC) and both correspond to a pure porous crystalline silicon dioxide. Experimental gas adsorption isotherms at cryogenic temperatures (i.e., 70-90-120 K) were performed in a volumetric analyzer (ASAP 2020 HD, Micromeritics) in the pressure range between  $10^{-2}$  and 120 kPa. The instrument was equipped with a turbo molecular vacuum pump and three pressure transducers (0.13, 1.33 and 133 kPa, uncertainty within 0.15% of each reading) to enhance the sensitivity in the low pressure range. Cryogenic temperatures were obtained using a helium cryocooler (Gifford-McMahon) coupled to the volumetric analyzer that allows a fine temperature control between 25–325 K with a stability of  $\pm 0.1$  K. Adsorption isotherms at 77 and 90 K were also measured using a liquid nitrogen and oxygen (respectively) bath to control the temperature; both sets of experimental data (cryocooler *vs* liquid nitrogen/oxygen) were found to be reproducible. Before the analysis, all zeolite powders were outgassed under dynamic vacuum at 623 K (1K/min) for overnight. All of the isotherms were done in triplicate and the data are reproducible with an error below 0.1%. All the gases were supplied by Air Products with an ultrahigh purity (i.e., 99.995%).

**Simulation methods and models.** To obtain the amount of adsorbed molecules in the zeolites we perform Monte Carlo simulations (MC) using the grand canonical ensemble where chemical potential, volume, and temperature are kept fixed. Fugacity is

obtained from the chemical potential, and it is directly related to pressure by the fugacity coefficient, using the Peng-Robinson equation of state. To compare with experimental data, simulated absolute adsorption isotherms are converted to excess adsorption isotherms as proposed by Duren *et al.*<sup>38</sup> Simulations are performed using the molecular simulation software RASPA.<sup>39</sup>

The zeolites used for the development and validation of the force fields are the pure silica versions of LTA (ITQ-29), FAU, and MFI and the aluminosilicate NaY with 54 sodium extra-framework cations. The frameworks are considered rigid. ITQ-29 was firstly synthesized by Corma *et al.*<sup>40</sup> with a cubic unit cell of 11.87 Å of side. For the pure silica FAU zeolite, we use the crystallographic position of the atoms reported by Hriljac *et al.*<sup>41</sup> with a cubic unit cell of  $a = b = c = 24.26$  Å. Both ITQ-29 and FAU are formed by sodalites connected to each other. To compare with other zeolite topology, pure silica MFI is also employed. This structure is characterized by the combination of longitudinal and zig-zag channels forming a 3D network. It is well known that MFI zeolite experiences phase transitions with loading and/or temperature.<sup>9,42-44</sup> These studies showed that the zeolite adopts a monoclinic configuration at temperature below 300 K, while above this temperature the symmetry changes to orthorhombic. For this reason and due to the fact that this study focuses on adsorption at low temperatures we use the monoclinic version of MFI zeolite as reported by van Koningsveld *et al.*<sup>45</sup> with unit cell of  $a = 20.12$  Å,  $b = 19.88$  Å and  $c = 13.37$  Å and  $\alpha = \gamma = 90^\circ$  and  $\beta = 90.67^\circ$ . To incorporate the effect of the presence of extra-framework cations and to parameterize the interactions of the cations with the adsorbates we compute adsorption in NaY (with 54 aluminum atoms and sodium cations per unit cell) using the crystallographic positions reported by Olson.<sup>46</sup> The low content of aluminum of this structure (54 per unit cell) avoids the possible formation of complexes between the

cations and the adsorbates.<sup>3,47-49</sup> NaY has a cubic unit cell with side size of 25.09 Å and the distribution of the aluminum atoms in our simulation cell obeys the Löwenstein rule that establish that the same oxygen atom cannot be connected to two aluminum atoms. Extra-framework cations are allowed to move during simulations, as it is known that their mobility has a strong effect on the adsorption behavior.<sup>2,3</sup>

Regarding adsorbates we use reported models for argon,<sup>50</sup> methane,<sup>1</sup> nitrogen,<sup>50</sup> oxygen,<sup>50</sup> and carbon monoxide<sup>51</sup>. Argon and methane are described as united atom models with Lennard-Jones parameters on a single interaction center.<sup>1,50</sup> Nitrogen, oxygen, and carbon monoxide are modelled with Lennard-Jones parameters, point charges in all their atoms<sup>50,51</sup> and charged dummy atoms without mass to reproduce the polarity of the molecules. All these models were fitted to reproduce experimental properties such as the vapor-liquid coexistence, vapor pressure, or liquid densities.

Guest-guest and host-guest interactions are modelled through Lennard-Jones and Coulombic interactions. Coulombic interactions are computed with the Ewald summation method with a relative precision of  $10^{-6}$ . Lennard-Jones potentials are cut and shifted with a cut-off distance of 12 Å. Van de Waals interactions between molecules are obtained from Lorentz-Berthelot mixing rules using already published parameters for the adsorbates.<sup>1,50,51</sup> As mentioned before, adsorbate-adsorbent interactions in zeolites do not obey generic mixing rules, therefore specific interactions need to be used. Usually, the dispersive interactions of silicon or aluminum atoms are considered through the oxygen atoms, acting these atoms as Lennard-Jones interacting centers. Nevertheless all the atoms of the system have partial charges assigned. In this work we use a set of charges for the structures that was previously reported by our group.<sup>8</sup> To define the Lennard-Jones interactions of the molecules with the structures,

we use published values for argon and methane<sup>1,9</sup> and we define new ones for nitrogen, oxygen, and carbon monoxide.

## Results

To obtain the parameters for the interactions of oxygen, nitrogen, and carbon monoxide with the zeolites, the first step is to reproduce the interaction of the gases in pure silica zeolites (gas- $O_{zeo}$ ). With this aim in mind we computed adsorption isotherms in ITQ-29 for all gases at 77 K, 90 K, and 120 K. The Lennard-Jones parameters between the oxygen atoms ( $O_{zeo}$ ) and the adsorbates were fitted to reproduce the experimental isotherms at the lowest temperature (77 K for oxygen and nitrogen and 120 K for carbon monoxide). In addition we compute adsorption isotherms at several temperatures to validate the fitted parameters that are collected in Table 1.

Table 1: Lennard-Jones parameters for guest-host interactions.

Atom 1	Atom 2	$\epsilon/k_B$ (K)	$\sigma$ (Å)
Ar	$O_{zeo}$	107.69	3.15
CH <sub>4</sub>	$O_{zeo}$	115	3.47
N <sub>2</sub>	$O_{zeo}$	60.58	3.261
O <sub>2</sub>	$O_{zeo}$	65.189	3.129
C <sub>CO</sub>	$O_{zeo}$	40.109	3.379
O <sub>CO</sub>	$O_{zeo}$	98.839	3.057
Ar	Na	262	2.396
CH <sub>4</sub>	Na	553.061	2.176
N <sub>2</sub>	Na	225.568	2.766
O <sub>2</sub>	Na	241.284	2.06
C <sub>CO</sub>	Na	369.343	2.332
O <sub>CO</sub>	Na	579.793	2.212



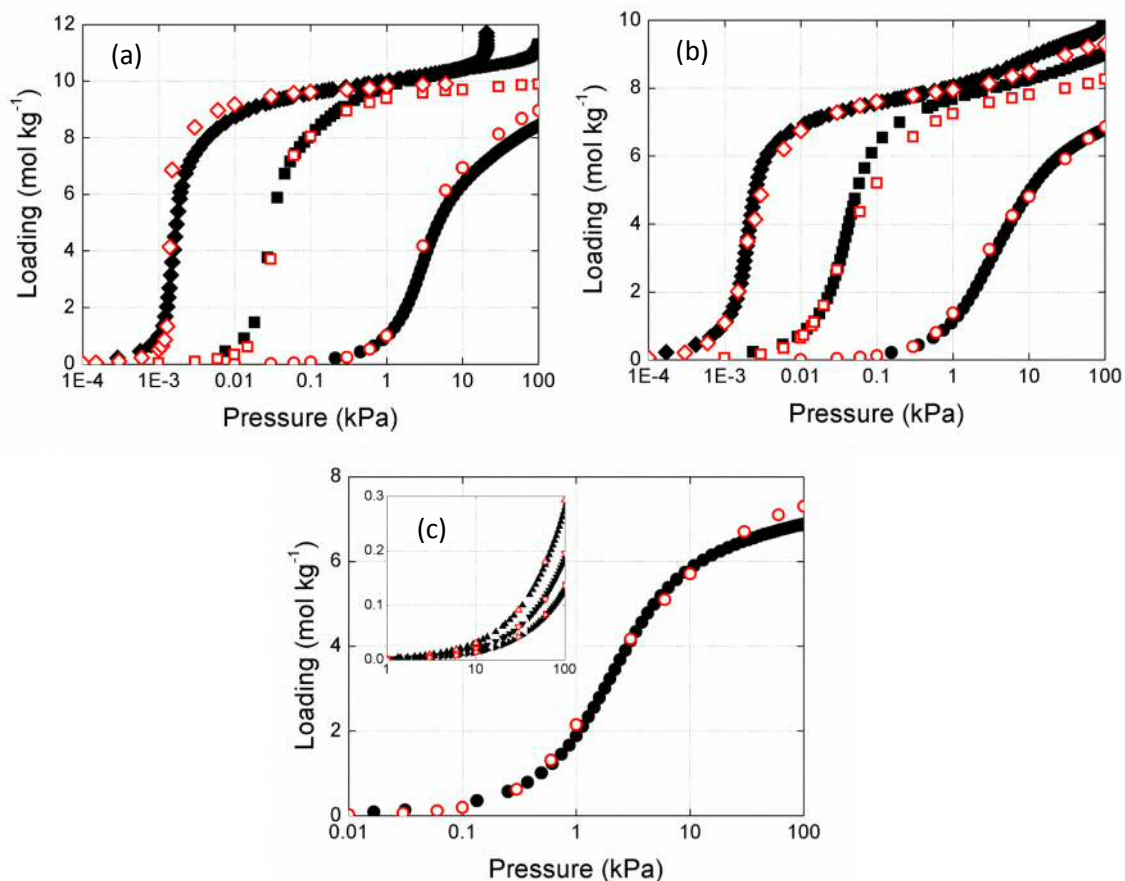


Figure 1: Experimental (full symbols) and computed (empty symbols) adsorption isotherms of (a) oxygen, (b), nitrogen, and (c) carbon monoxide in ITQ-29 at 77 K (rhombus), 90 K (squares), and 120 K (circles). The inset in Fig. 1c shows isotherms at 258 K, 278 K, and 298 K (up-, down-, and right-triangles, respectively) in the same units as the main graph. Computed adsorption isotherms show the excess loading for a better comparison with experiments.

The force field parameters for argon and methane, taken from the literature,<sup>1,9</sup> have also been validated to reproduce experimental adsorption at low temperature (120 K). As shown in Figure S1 from the Electronic Supporting Information (ESI) simulations reproduce experimental adsorption accurately.

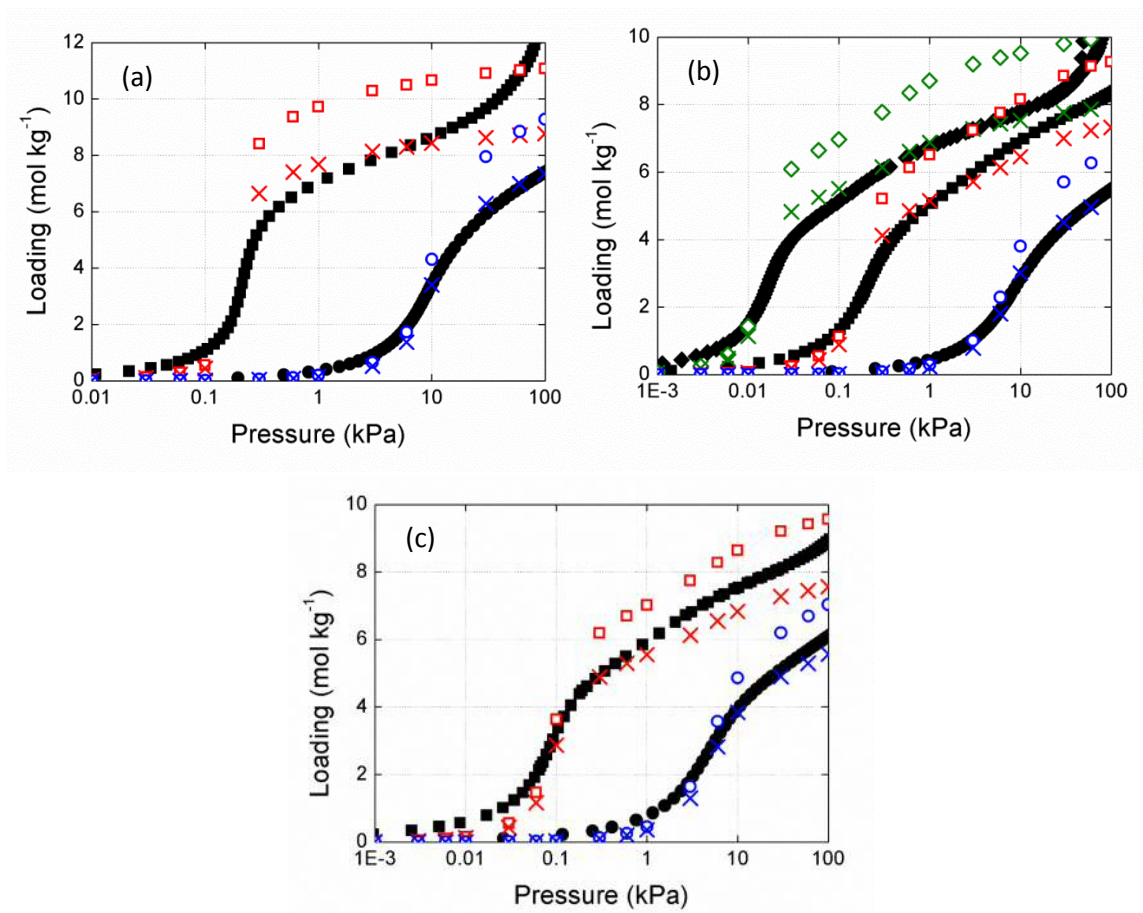


Figure 2: Experimental (full symbols) and computed (empty symbols) adsorption isotherms for (a) oxygen, (b) nitrogen and (c) carbon monoxide in pure silica FAU at 77 K (rhombus), 90 K (squares) and 120 K (circles). Crosses indicate theoretical adsorption after the correction applied as a result of the different surface areas. Computed adsorption isotherms show the excess loading for a better comparison with experiments.

To analyze the transferability of the new set of parameters, adsorption isotherms were computed for other pure silica zeolites. Figure 2 shows the adsorption isotherms computed for pure silica FAU zeolite, compared to experimental data obtained in CBV901 (nearly pure silica FAU zeolite) at different temperatures. As observed in this figure the results obtained from simulations successfully reproduce experimental data at

low and medium values of pressure. The main discrepancies are observed at high pressure, where the experimental adsorption is lower than the simulated. This is due to the fact that the zeolite used in the experimental measurements (CBV901) has a surface area of 700 m<sup>2</sup>/g while the structure used for the molecular simulations has a surface area of 885 m<sup>2</sup>/g. Therefore the saturation capacity is larger for the latter than for the former. To validate this reasoning a correction factor of 0.79 is applied to the simulation results, obtaining the proper agreement with the experimental values. This correction is not needed in the case of ITQ-29 as the computed and the experimental surface areas are very similar (773 m<sup>2</sup>/g and 800 m<sup>2</sup>/g, respectively). Since ITQ-29 and FAU contain sodalite cages connected to each other, adsorption isotherms have also been obtained for pure silica MFI zeolite in order to check transferability of our parameters to other topologies. Figure 3 compares experimental and computed adsorption isotherms obtained for oxygen, nitrogen, and carbon monoxide in pure silica MFI zeolite (experimental RSIL). As can be noted the lowest temperature brings some discrepancies that we attribute to difficulties to reach real equilibrium conditions at such low temperatures in this zeolite (supported by the steep adsorption at low pressures). Another example is given in Figure 4, showing the adsorption isotherms of nitrogen in pure silica MFI at 77 K and pointing out a disagreement in the experimental data provided by different authors.<sup>52,53</sup> As it can be seen, our experimental isotherm is in agreement with the previously reported by Nakai *et al.*<sup>52</sup> However it shows large discrepancies with the isotherms reported by Hammond *et al.*<sup>53</sup> at low pressures, though the three of them exhibit the same saturation capacity. This should be attributed to the lack of sensitivity in the low pressure region (below 1\*10<sup>-6</sup> kPa) of the instruments, both gravimetric and volumetric, used for recording the experimental data.<sup>53</sup> Back to Figure 3, depending on the adsorbate, differences between experiments and simulations can be

found at temperature below 77 K (oxygen) or 90 K (nitrogen and carbon monoxide). Discrepancies observed for MFI were not found for previous zeolites (ITQ-29 and FAU). These differences could be due to phase transition on the MFI structure as well as to differences on the size of the crystals used in the experimental samples. Experimental isotherms recorded on MFI with different crystal sizes (data not shown) were found to be similar, thus suggesting the phase transition in MFI as the main factor accounting for the differences observed in Figure 3. The changes on the zeolite may affect to the limiting effective size of the structure, being the effect more visible on the adsorption of the largest molecules (nitrogen and carbon monoxide). Additional comparison with previous works in MFI for nitrogen, carbon monoxide, and argon at high temperature (305-343 K)<sup>54,55</sup> are shown in Figures S2-S4 in ESI.

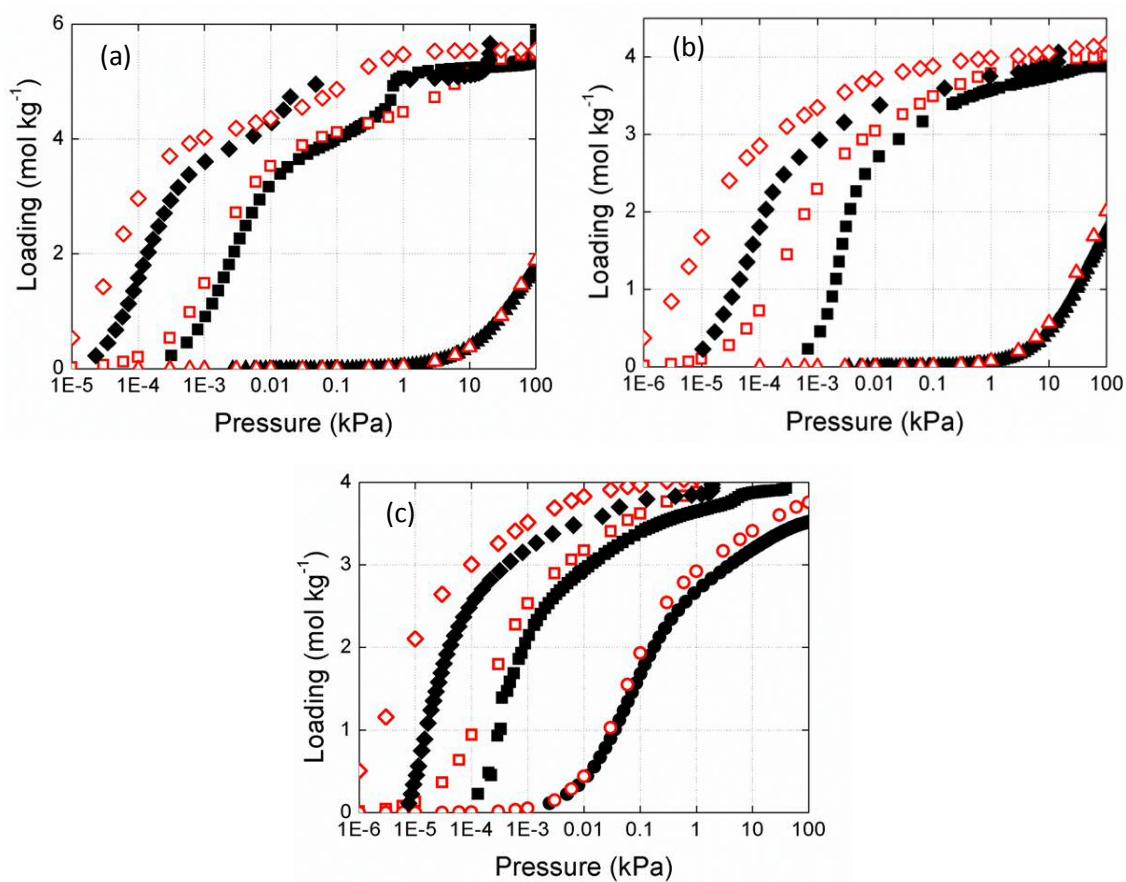


Figure 3: Experimental (full symbols) and computed (empty symbols) adsorption isotherms for (a) oxygen, (b) nitrogen and (c) carbon monoxide in pure silica MFI at 77 K (rhombus), 90 K (squares), 120 K (circles) and 196 K (triangles). Computed adsorption isotherms show the excess loading for a better comparison with experiments.

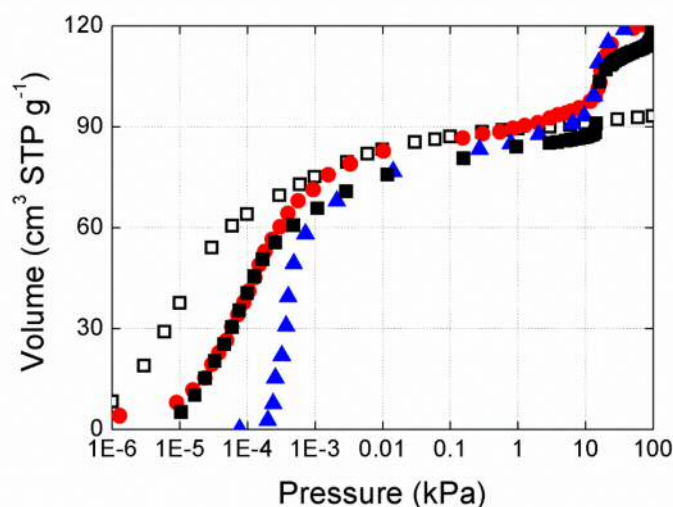


Figure 4: Adsorption isotherms of nitrogen in pure silica MFI at 77 K. The experimental data (solid symbols) obtained in this work (squares) are compared with available data provided by Nakai *et al.*<sup>52</sup> (circles) and Hammond *et al.*<sup>53</sup> (triangles). Empty squares correspond to the adsorption isotherm that we have obtained from simulations. Computed adsorption isotherms show the excess loading for a better comparison with experiments.

The presence of aluminum in the structures (location and density) and the type of extra-framework cation highly influences adsorption. In structures with Si/Al ratio close to 1, such as LTA4A, the basicity of the oxygen atoms and the number of sodium extra-framework cations lead to the formation of carbonate-like-species during the adsorption of molecules such as carbon dioxide and carbon monoxide.<sup>3,56</sup> These complexes affect the accessible volume of the structure and the interactions with the molecules. We have recently reported a work dealing with the formation of these complexes in LTA4A zeolites<sup>3</sup> and we are currently working on the development of a similar set of parameters involving the formation of carbonate-like species between

carbon monoxide and this particular structure. Molecules such as nitrogen, argon, methane, or oxygen are not able to enter the LTA4A structure due to kinetic restrictions.<sup>57,58</sup> Hence, to study the effect of the presence of cations avoiding the problems afore mentioned we focus on NaY zeolite with 54 sodium cations per unit cell (u.c.). Using similar procedure as for pure silica zeolites we use our experimental isotherms to fit the Lennard-Jones parameters between the adsorbates and sodium cations and to validate these parameters.

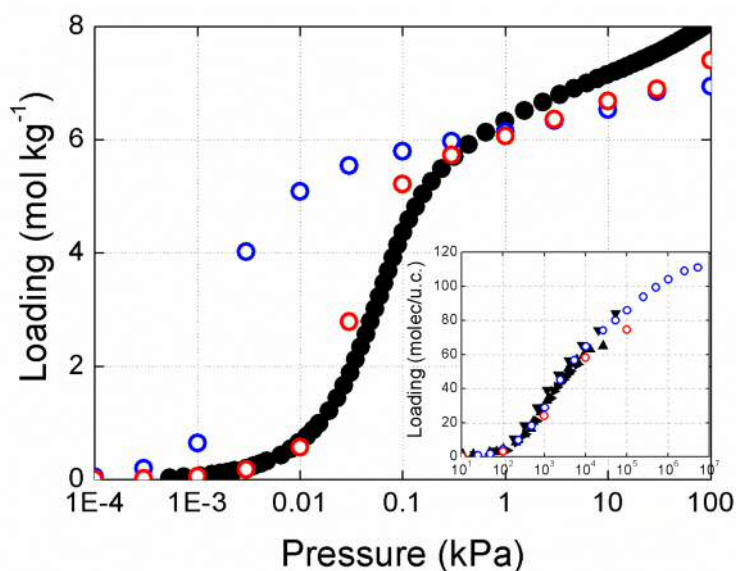


Figure 5: Experimental (full symbols) and computed (empty symbols) adsorption isotherms of methane in NaY (54 Na<sup>+</sup>/u.c.) at 120 K. Blue symbols correspond to the results obtained using the parameters reported by Calero *et al.*<sup>2</sup>, and red symbols to the ones obtained after fitting these parameters. The inset shows a comparison of methane adsorption isotherms in FAU (48 Na<sup>+</sup>/u.c.) at 323 K with experimental values from Rowlinson, Fuchs and Talu as shown in the publication of Calero *et al.*<sup>2</sup> Computed adsorption isotherms show the excess loading for a better comparison with experiments.

Unfortunately, there is still a big lack of force fields in zeolites containing non-framework cations. Among the gases under study and to the best of our knowledge, there is only one set of parameters for methane.<sup>2</sup> These parameters were optimized and validated for adsorption in FAU-type zeolites at temperatures spanning from 298 K to 330 K. As shown in Figure 5 these parameters fail to reproduce adsorption at 120 K, since it overestimates the uptake at low pressures. However the saturation obtained by simulation is in reasonably good agreement with the experimental data. Amazingly enough, slight variations on the epsilon and sigma parameters lead to reproduce the experimental adsorption isotherms at low and high temperatures. This evidences the large sensitivity of the Lennard-Jones parameters when the adsorption isotherm is computed at low temperature. In addition, it is possible to find disagreements between experiments and simulations at low and medium values of pressure due to another two factors (Figure 6). On the one hand, we can find experimental restrictions similar to these observed at 77 K for pure silica structures. On the other hand the lowest uptake obtained in the experiments could be also attributed to kinetic effects. At low temperatures the reduced mobility of the cations could lead them to block the windows that communicate the  $\alpha$ -cages of faujasite. Therefore higher pressures are needed for the molecule to enter the structure. This kinetic restriction disappears at higher temperatures allowing good agreement between experiments and simulations at temperatures above 90 K. To avoid kinetic impedimenta, the Lennard-Jones parameters that describe the interactions of nitrogen, oxygen, carbon monoxide, and argon with the sodium cation were fitted to the experimental isotherms obtained at 120 K and validated at higher and lower temperatures. As shown in Figure 6, the experimental and simulated adsorption isotherms at temperatures above 90 K for oxygen (6a), nitrogen (6b), and carbon monoxide (6c) are in very good agreement. However, simulation fails to reproduce



experiment at lower temperatures. These discrepancies do not apply to argon (Figure 6d) since the interaction of this gas with the cations is quite weak and therefore the adsorption of this molecule is not affected by kinetic restrictions.

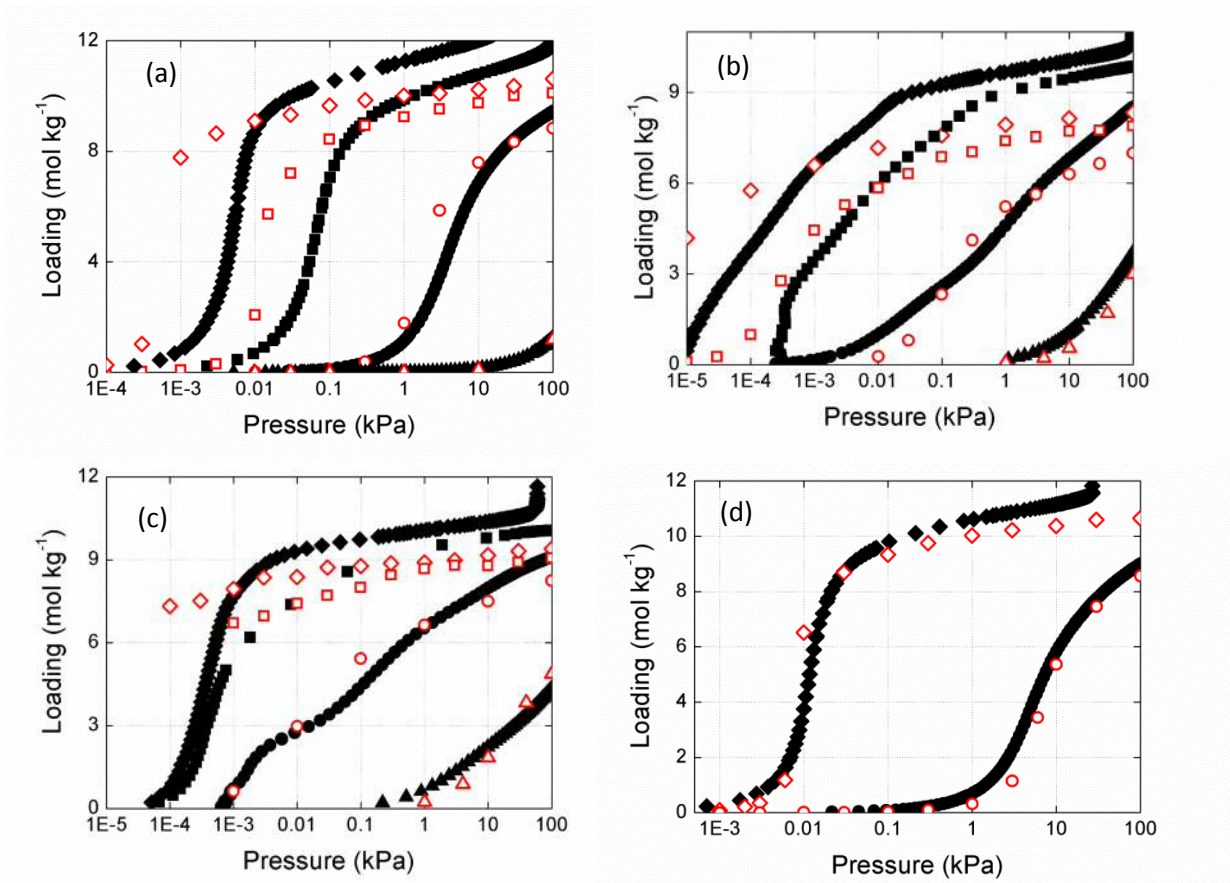


Figure 6: Experimental (full symbols) and computed (empty symbols) adsorption isotherms of a) oxygen, b) nitrogen, c) carbon monoxide and d) argon in NaY (54 Na+/u.c.) at 77 K (rhombus), 90 K (squares), 120 K (circles) and 196 K (triangles). Computed adsorption isotherms show the excess loading for a better comparison with experiments.

As previously done for the pure silica zeolites, we validate the transferability of the interaction parameters of the gases with sodium extra-framework cation by comparison with experimental adsorption values in zeolites with different Si/Al ratio and topology. With this aim we compute adsorption isotherms of O<sub>2</sub>, N<sub>2</sub>, Ar, and CH<sub>4</sub> in NaX (Si/Al=1.23) and Na-MFI (Si/Al=30) at room temperature, and compare them with the results reported by Dunne *et al.*<sup>59</sup> As observed in Figures S5-S8 from the ESI, the agreement obtained in both structures is really accurate, proving therefore the transferability of the proposed parameters.

## Conclusions

We analyzed the effect of temperature on the adsorption behavior of argon, methane, nitrogen, oxygen, and carbon monoxide in both pure silica and aluminosilicate zeolites. To this aim the development of new sets of transferable parameters was needed. These parameters are of key importance to perform adsorption studies by molecular simulation as generic mixing rules fail to reproduce adsorption in zeolitic systems and previous works with specific parameters are scarce. The new sets of parameters are compatible to these previously reported for carbon dioxide, methane, and argon opening the possibility of studying mixtures of all components. We found that some systems need very low pressures to reach equilibrium and experimental devices are not always able to reach such pressures leading in this case to erroneous isotherms. When cations are involved in the system the low temperature affects their mobility being needed higher pressures to allow molecules to enter the structures. This kinetic effect cannot be mimicked using Monte Carlo simulations being therefore more difficult to reproduce experimental results.

## ACKNOWLEDGEMENTS

This work was supported by the European Research Council through an ERC Staring Grant (ERC-StG-279520-RASPA). A. Martín-Calvo thanks the Spanish “Ministerio de Educación Cultura y Deporte” for her predoctoral fellowship. The authors want to thank the “Instituto de Tecnología Química” (ITQ-CSIC) from Valencia, for providing the pure silica zeolites (RSIL and ITQ-29).

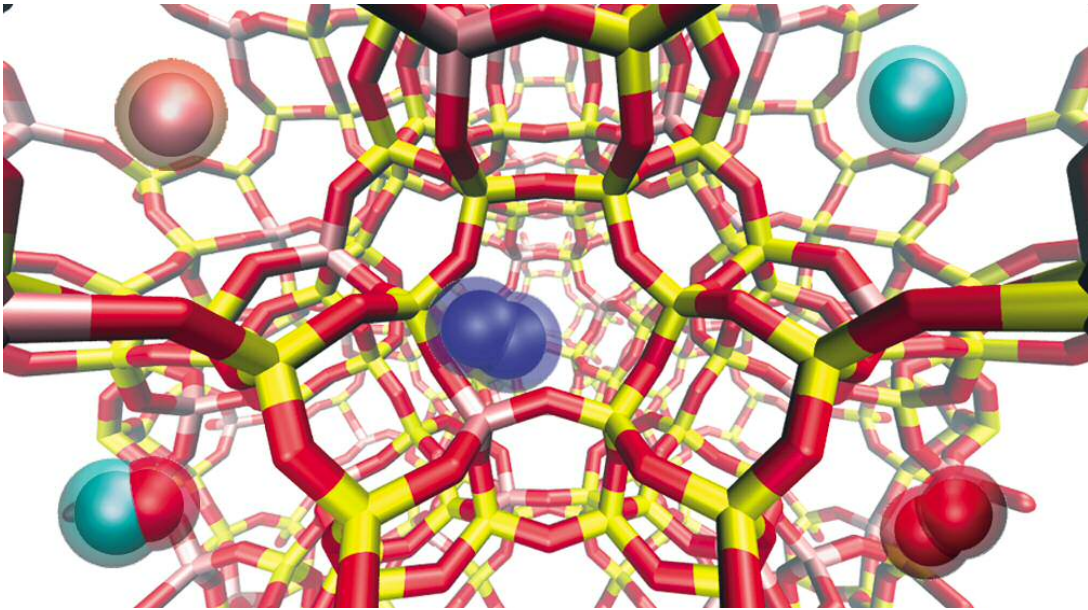
## REFERENCES

- (1) Dubbeldam, D.; Calero, S.; Vlugt, T. J. H.; Krishna, R.; Maesen, T. L. M.; Smit, B. *Journal of Physical Chemistry B* **2004**, *108*, 12301.
- (2) Calero, S.; Dubbeldam, D.; Krishna, R.; Smit, B.; Vlugt, T. J. H.; Denayer, J. F. M.; Martens, J. A.; Maesen, T. L. M. *Journal of the American Chemical Society* **2004**, *126*, 11377.
- (3) Martín-Calvo, A.; Parra, J. B.; Ania, C. O.; Calero, S. *Journal of Physical Chemistry C* **2014**, *118*, 25460.
- (4) Dueren, T.; Bae, Y.-S.; Snurr, R. Q. *Chemical Society Reviews* **2009**, *38*, 1237.
- (5) Bueno-Perez, R.; Calero, S.; Dubbeldam, D.; Ania, C. O.; Parra, J. B.; Zaderenko, A. P.; Merklung, P. J. *Journal of Physical Chemistry C* **2012**, *116*, 25797.
- (6) Balestra, S. R. G.; Gutierrez-Sevillano, J. J.; Merklung, P. J.; Dubbeldam, D.; Calero, S. *Journal of Physical Chemistry C* **2013**, *117*, 11592.
- (7) Dubbeldam, D.; Calero, S.; Vlugt, T. J. H.; Krishna, R.; Maesen, T. L. M.; Beerdsen, E.; Smit, B. *Physical Review Letters* **2004**, *93*.
- (8) Garcia-Sanchez, A.; Ania, C. O.; Parra, J. B.; Dubbeldam, D.; Vlugt, T. J. H.; Krishna, R.; Calero, S. *Journal of Physical Chemistry C* **2009**, *113*, 8814.
- (9) Garcia-Perez, E.; Parra, J. B.; Ania, C. O.; Dubbeldam, D.; Vlugt, T. J. H.; Castillo, J. M.; Merklung, P. J.; Calero, S. *Journal of Physical Chemistry C* **2008**, *112*, 9976.
- (10) Goj, A.; Sholl, D. S.; Akten, E. D.; Kohen, D. *Journal of Physical Chemistry B* **2002**, *106*, 8367.
- (11) Makrodimitris, K.; Papadopoulos, G. K.; Theodorou, D. N. *Journal of Physical Chemistry B* **2001**, *105*, 777.
- (12) Hirotani, A.; Mizukami, K.; Miura, R.; Takaba, H.; Miya, T.; Fahmi, A.; Stirling, A.; Kubo, M.; Miyamoto, A. *Applied Surface Science* **1997**, *120*, 81.
- (13) Li, P.; Tezel, F. H. *Journal of Chemical and Engineering Data* **2008**, *53*, 2479.

- (14) Jaramillo, E.; Chandross, M. *Journal of Physical Chemistry B* **2004**, *108*, 20155.
- (15) Akten, E. D.; Siriwardane, R.; Sholl, D. S. *Energy & Fuels* **2003**, *17*, 977.
- (16) Maurin, G.; Llewellyn, P. L.; Bell, R. G. *Journal of Physical Chemistry B* **2005**, *109*, 16084.
- (17) Madison, L.; Heitzer, H.; Russell, C.; Kohen, D. *Langmuir* **2011**, *27*, 1954.
- (18) Babarao, R.; Jiang, J. *Langmuir* **2008**, *24*, 5474.
- (19) Krishna, R.; van Baten, J. M. *Journal of Membrane Science* **2010**, *360*, 323.
- (20) Krishna, R.; van Baten, J. M. *Microporous and Mesoporous Materials* **2008**, *109*, 91.
- (21) Garcia-Perez, E.; Parra, J. B.; Ania, C. O.; Garcia-Sanchez, A.; Van Baten, J. M.; Krishna, R.; Dubbeldam, D.; Calero, S. *Adsorption-Journal of the International Adsorption Society* **2007**, *13*, 469.
- (22) Garcia-Sanchez, A.; van den Bergh, J.; Castillo, J. M.; Calero, S.; Kapteijn, F.; Vlugt, T. J. H. *Microporous and Mesoporous Materials* **2012**, *158*, 64.
- (23) Garcia-Sanchez, A.; Garcia-Perez, E.; Dubbeldam, D.; Krishna, R.; Calero, S. *Adsorption Science & Technology* **2007**, *25*, 417.
- (24) Pillai, R. S.; Sethia, G.; Jasra, R. V. *Industrial & Engineering Chemistry Research* **2010**, *49*, 5816.
- (25) Martin, M. G.; Siepmann, J. I. *Journal of Physical Chemistry B* **1998**, *102*, 2569.
- (26) Krishna, R.; van Baten, J. M.; Garcia-Perez, E.; Calero, S. *Chemical Physics Letters* **2006**, *429*, 219.
- (27) Fritzsche, S.; Haberlandt, R.; Hofmann, G.; Karger, J.; Heinzinger, K.; Wolfsberg, M. *Chemical Physics Letters* **1997**, *265*, 253.
- (28) Leroy, F.; Jobic, H. *Chemical Physics Letters* **2005**, *406*, 375.
- (29) Zimmermann, N. E. R.; Jakobtorweihen, S.; Beerdsen, E.; Smit, B.; Keil, F. J. *Journal of Physical Chemistry C* **2007**, *111*, 17370.
- (30) Dubbeldam, D.; Smit, B. *Journal of Physical Chemistry B* **2003**, *107*, 12138.
- (31) Cho, H. S.; Miyasaka, K.; Kim, H.; Kubota, Y.; Takata, M.; Kitagawa, S.; Ryoo, R.; Terasaki, O. *Journal of Physical Chemistry C* **2012**, *116*, 25300.
- (32) Pillai, R. S.; Sebastian, J.; Jasra, R. V. *Journal of Porous Materials* **2012**, *19*, 683.
- (33) Sethia, G.; Pillai, R. S.; Dangi, G. P.; Somani, R. S.; Bajaj, H. C.; Jasra, R. V. *Industrial & Engineering Chemistry Research* **2010**, *49*, 2353.
- (34) Sebastian, J.; Pillai, R. S.; Peter, S. A.; Jasra, R. V. *Industrial & Engineering Chemistry Research* **2007**, *46*, 6293.
- (35) Mellot, C.; Lignieres, J. *Molecular Simulation* **1996**, *18*, 349.
- (36) Nour, Z.; Berthomieu, D.; Yang, Q.; Maurin, G. *Journal of Physical Chemistry C* **2012**, *116*, 24512.
- (37) Wang, Y.; Helvensteijn, B.; Nizamidin, N.; Erion, A. M.; Steiner, L. A.; Mulloth, L. M.; Luna, B.; LeVan, M. D. *Langmuir* **2011**, *27*, 10648.
- (38) Duren, T.; Sarkisov, L.; Yaghi, O. M.; Snurr, R. Q. *Langmuir* **2004**, *20*, 2683.
- (39) Dubbeldam, D.; Calero, S.; Donald, E.; Snurr, R. Q. *Molecular Simulation* **2015**, DOI:10.1080/08927022.2015.1010082.

- (40) Corma, A.; Rey, F.; Rius, J.; Sabater, M. J.; Valencia, S. *Nature* **2004**, *431*, 287.
- (41) Hriljac, J. A.; Eddy, M. M.; Cheetham, A. K.; Donohue, J. A.; Ray, G. J. *Journal of Solid State Chemistry* **1993**, *106*, 66.
- (42) Hay, D. G.; Jaeger, H. *Journal of the Chemical Society-Chemical Communications* **1984**, 1433.
- (43) Fyfe, C. A.; Strobl, H.; Kokotailo, G. T.; Kennedy, G. J.; Barlow, G. E. *Journal of the American Chemical Society* **1988**, *110*, 3373.
- (44) Wu, E. L.; Lawton, S. L.; Olson, D. H.; Rohrman, A. C.; Kokotailo, G. T. *Journal of Physical Chemistry* **1979**, *83*, 2777.
- (45) Vankoningsveld, H.; Jansen, J. C.; Vanbekkum, H. *Zeolites* **1990**, *10*, 235.
- (46) Olson, D. H. *Zeolites* **1995**, *15*, 439.
- (47) Jacobs, P. A.; Vancauwe.Fh; Vansant, E. F.; Uytterho.Jb *Journal of the Chemical Society-Faraday Transactions I* **1973**, *69*, 1056.
- (48) Jacobs, P. A.; Vancauwe.Fh; Vansatn, E. F. *Journal of the Chemical Society-Faraday Transactions I* **1973**, *69*, 2130.
- (49) Martra, G.; Coluccia, S.; Davit, P.; Gianotti, E.; Marchese, L.; Tsuji, H.; Hattori, H. *Research on Chemical Intermediates* **1999**, *25*, 77.
- (50) Martin-Calvo, A.; Garcia-Perez, E.; Garcia-Sanchez, A.; Bueno-Perez, R.; Hamad, S.; Calero, S. *Physical Chemistry Chemical Physics* **2011**, *13*, 11165.
- (51) Martin-Calvo, A.; Lahoz-Martin, F. D.; Calero, S. *Journal of Physical Chemistry C* **2012**, *116*, 6655.
- (52) Nakai, K.; Sonoda, J.; Yoshida, M.; Hakuman, M.; Naono, H. *Adsorption-Journal of the International Adsorption Society* **2007**, *13*, 351.
- (53) Hammond, K. D.; Tompsett, G. A.; Auerbach, S. M.; Conner, W. C., Jr. *Langmuir* **2007**, *23*, 8371.
- (54) Dunne, J. A.; Mariwals, R.; Rao, M.; Sircar, S.; Gorte, R. J.; Myers, A. L. *Langmuir* **1996**, *12*, 5888.
- (55) Golden, T. C.; Sircar, S. *Journal of Colloid and Interface Science* **1994**, *162*, 182.
- (56) Arean, C. O.; Delgado, M. R.; Bauca, C. L.; Vrbka, L.; Nachtigall, P. *Physical Chemistry Chemical Physics* **2007**, *9*, 4657.
- (57) Eagan, J. D.; Anderson, R. B. *Journal of Colloid and Interface Science* **1975**, *50*, 419.
- (58) Arkharov, A. M.; Bering, B. P.; Kalinnikova, I. A.; Serpinskii, V. V. *Russian Chemical Bulletin* **1972**, *21*, 1389.
- (59) Dunne, J. A.; Rao, M.; Sircar, S.; Gorte, R. J.; Myers, A. L. *Langmuir* **1996**, *12*, 5896.

TOC



# Supporting Information

## Transferable Force Field for Adsorption of Small Gases in Zeolites

*A. Martin-Calvo<sup>1</sup>, J. J. Gutiérrez-Sevillano<sup>1</sup>, J. B. Parra<sup>2</sup>, C.O. Ania<sup>2</sup>, and S. Calero<sup>1\*</sup>*

<sup>1</sup>Department of Physical, Chemical, and Natural Systems, University Pablo de Olavide,  
Ctra. de Utrera, km. 1, 41013 Seville, Spain

<sup>2</sup> *Instituto Nacional del Carbón, INCAR-CSIC, P.O. 73, 33080 Oviedo, Spain*

\*Correspondence should be addressed to S. Calero (scalero@upo.es)



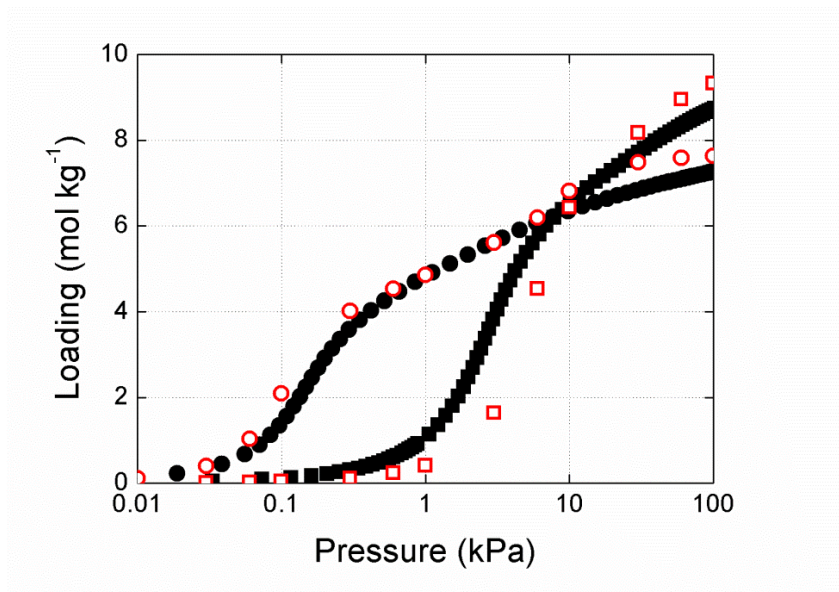


Figure S1: Experimental (full symbols) and computed (empty symbols) adsorption isotherms of argon (squares) and methane (circles) in ITQ-29 at 120 K. Computed adsorption isotherms show the excess loading for a better comparison with experiments.

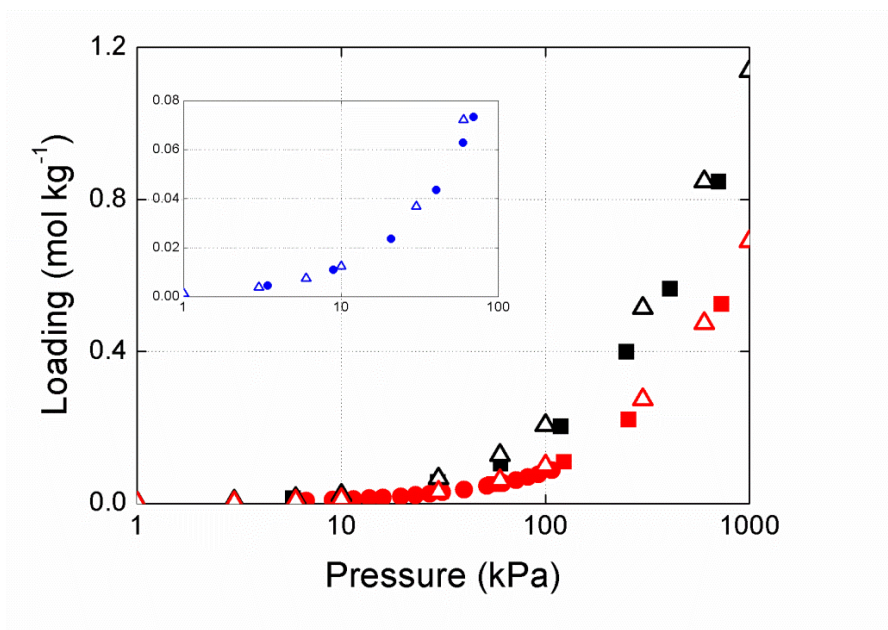


Figure S2: Experimental (full symbols) and computed (empty symbols) adsorption isotherms of nitrogen in pure silica MFI at 305K (black), 334 K (blue) and 343 K (red). Available data from Dunne *et al.*<sup>1</sup> (circles), and Golden and Sircar<sup>2</sup> [ENREF\\_2](#) (squares) are included for comparison. Computed adsorption isotherms show the excess loading for a better comparison with experiments.



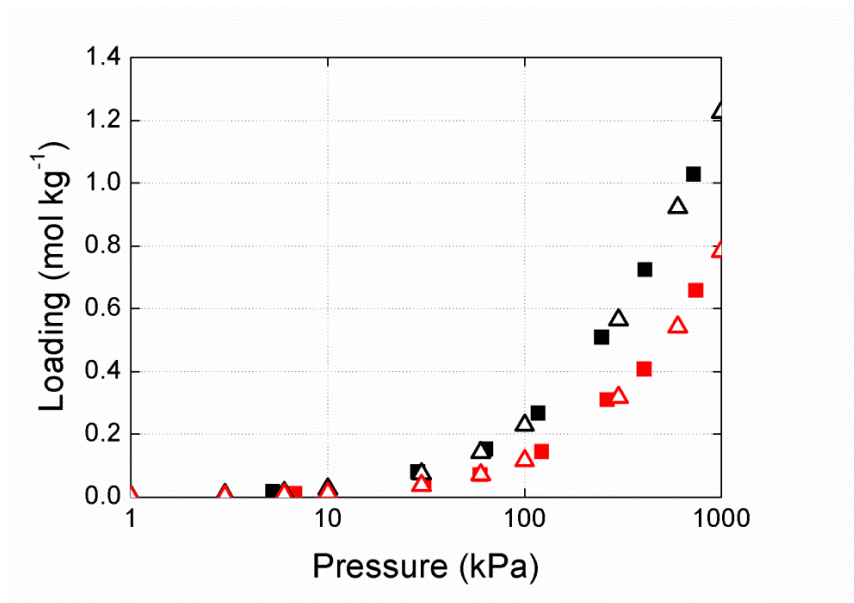


Figure S3: Experimental (full symbols) and computed (empty symbols) adsorption isotherms of carbon monoxide in MFI at 305K (black) and 341 K (red). Available data from Golden and Sircar<sup>2</sup> (squares) are included for comparison. Computed adsorption isotherms show the excess loading for a better comparison with experiments.

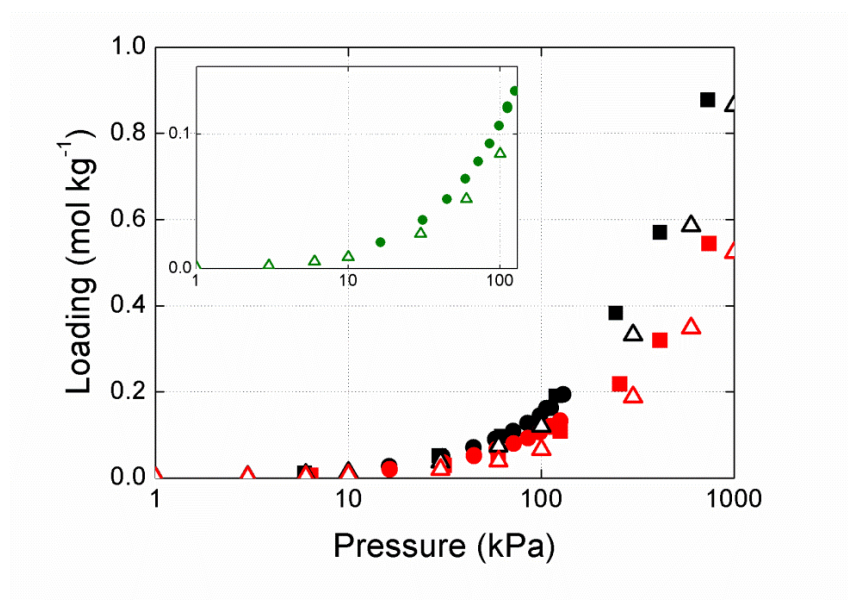


Figure S4: Experimental (full symbols) and computed (empty symbols) adsorption isotherms of argon in MFI at 305K (black), 325 K (green) and 342 K (red). Available data from Dunne *et al.*<sup>1</sup> (circles), and Golden and Sircar<sup>2</sup> (squares) are included for comparison. Computed adsorption isotherms show the excess loading for a better comparison with experiments.

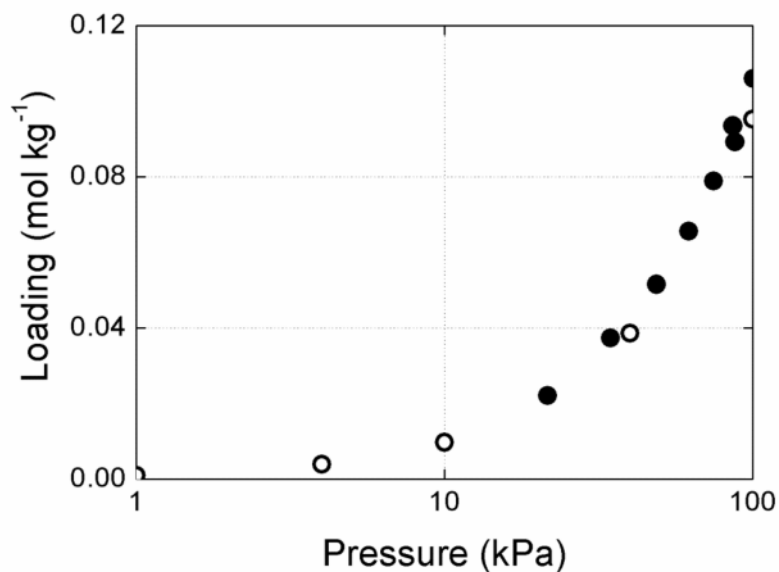


Figure S5: Experimental (full symbols) and computed (empty symbols) adsorption isotherms of oxygen in NaX Si/Al ratio=1.23 at 305 K (circles). Available data from Dunne *et al.*<sup>3</sup> are included for comparison. Computed adsorption isotherms show the excess loading for a better comparison with experiments.

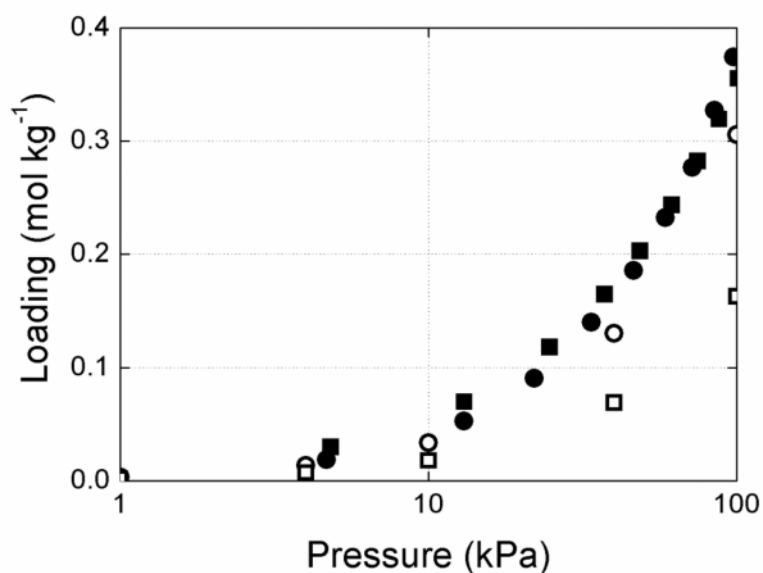


Figure S6: Experimental (full symbols) and computed (empty symbols) adsorption isotherms of nitrogen in NaX Si/Al ratio=1.23 at 305 K (circles), and Na-MFI Si/Al ratio=30 at 295 K. (squares) Available data from Dunne *et al.*<sup>3</sup> are included for comparison. Computed adsorption isotherms show the excess loading for a better comparison with experiments.

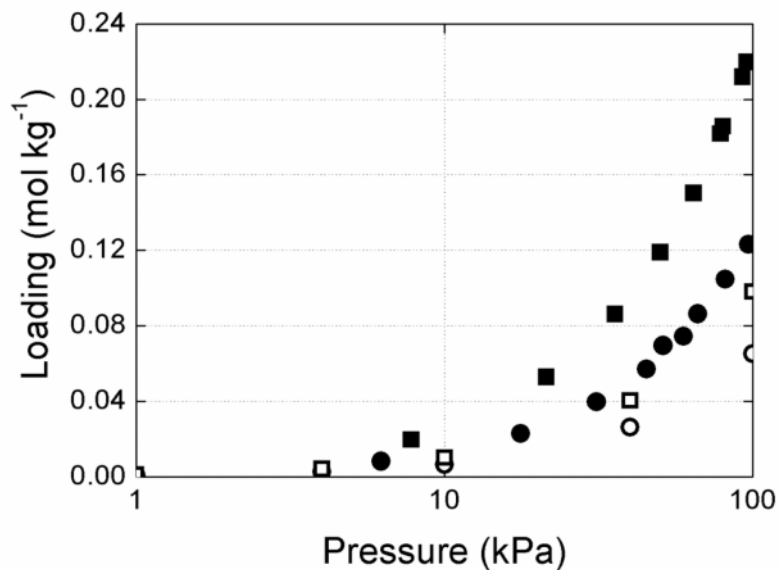


Figure S7: Experimental (full symbols) and computed (empty symbols) adsorption isotherms of argon in NaX Si/Al ratio=1.23 at 305 K (circles), and Na-MFI Si/Al ratio=30 at 295 K. (squares) Available data from Dunne *et al.*<sup>3</sup> are included for comparison. Computed adsorption isotherms show the excess loading for a better comparison with experiments.

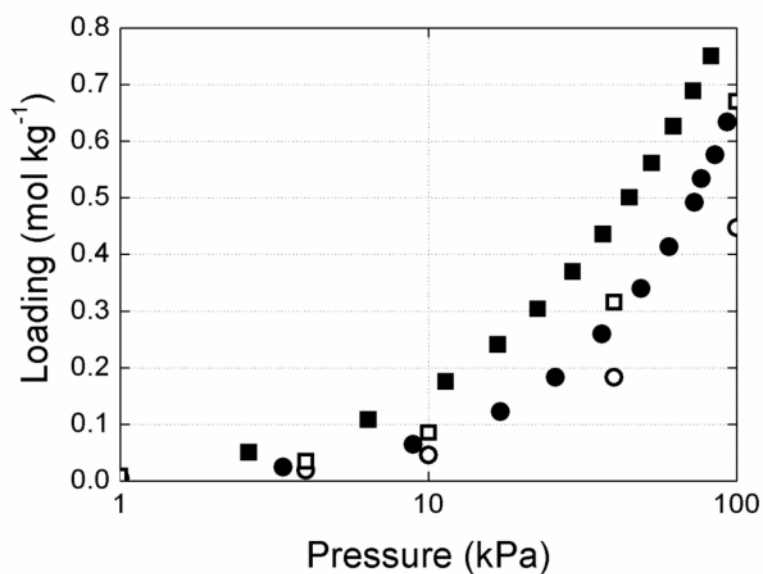


Figure S8: Experimental (full symbols) and computed (empty symbols) adsorption isotherms of methane in NaX Si/Al ratio=1.23 at 305 K (circles), and Na-MFI Si/Al ratio=30 at 295 K. (squares) Available data from Dunne *et al.*<sup>3</sup> are included for comparison. Computed adsorption isotherms show the excess loading for a better comparison with experiments.

- (1) Dunne, J. A.; Mariwals, R.; Rao, M.; Sircar, S.; Gorte, R. J.; Myers, A. L., Calorimetric Heats of Adsorption and Adsorption Isotherms .1. O-2, N-2, Ar, Co2, Ch4, C2h6 and Sf6 on Silicalite. *Langmuir*. **1996**, *12*, 5888-5895.
- (2) Golden, T. C.; Sircar, S., Gas-Adsorption on Silicalite. *Journal of Colloid and Interface Science*. **1994**, *162*, 182-188.
- (3) Dunne, J. A.; Rao, M.; Sircar, S.; Gorte, R. J.; Myers, A. L., Calorimetric Heats of Adsorption and Adsorption Isotherms .2. O-2, N-2, Ar, Co2, Ch4, C2h6, and Sf6 on Nax, H-Zsm-5, and Na-Zsm-5 Zeolites. *Langmuir*. **1996**, *12*, 5896-5904.